



PAPER

Interaction potentials, electric moments, polarizabilities, and chemical reactions of YbCu, YbAg, and YbAu molecules

OPEN ACCESS

RECEIVED
23 May 2021REVISED
18 July 2021ACCEPTED FOR PUBLICATION
21 July 2021PUBLISHED
9 August 2021

Original content from
this work may be used
under the terms of the
[Creative Commons
Attribution 4.0 licence](#).

Any further distribution
of this work must
maintain attribution to
the author(s) and the
title of the work, journal
citation and DOI.



Michał Tomza*

Faculty of Physics, University of Warsaw, Pasteura 5, 02-093 Warsaw, Poland

* Author to whom any correspondence should be addressed.

E-mail: michal.tomza@fuw.edu.pl**Keywords:** ultracold molecules, interatomic interaction potentials, electric moments, polarizabilities, ultracold chemical reactions, electronic structure calculationsSupplementary material for this article is available [online](#)**Abstract**

Ultracold YbAg molecules have been recently proposed as promising candidates for electron electric dipole moment searches Verma *et al* (2020 *Phys. Rev. Lett.* **125** 153201). Here, we calculate potential energy curves, permanent electric dipole and quadrupole moments, and static electric dipole polarizabilities for the YbCu, YbAg, and YbAu molecules in their ground electronic states. We use the coupled cluster method restricted to single, double, and noniterative triple excitations with large Gaussian basis sets, while the scalar relativistic effects are included within the small-core energy-consistent pseudopotentials. We find that the studied molecules are relatively strongly bound with the well depths of 5708 cm^{-1} , 5253 cm^{-1} , and 13349 cm^{-1} and equilibrium distances of 5.50 bohr, 5.79 bohr, and 5.55 bohr for YbCu, YbAg, and YbAu, respectively. They have large permanent electric dipole moments of $3.2D$, $3.3D$, and $5.3D$ at equilibrium distances, respectively. We also calculate equilibrium geometries and energies of corresponding trimers. The studied molecules are chemically reactive unless they are segregated in an optical lattice or shielded with external fields. The investigated molecules may find application in ultracold controlled chemistry, dipolar many-body physics, or precision measurement experiments.

1. Introduction

Ultracold polar molecules constitute excellent systems for studying the fundamentals of quantum physics and chemistry [1]. Rich and controllable internal molecular structure and intermolecular interactions allow for unique experiments on ultracold controlled chemistry [2], quantum simulations of many-body physics [3], and precision measurements [4]. Highly accurate molecular spectroscopy can be employed to probe fundamental physics, including tests of fundamental symmetries [5], searches for the spatiotemporal variation of fundamental constants [6], measurements of the electric dipole moment of the electron [7], the electron-to-proton mass ratio or the fine structure constant [8], tests of quantum electrodynamics [8], and others [9].

Recently, ultracold RaAg [10, 11] and YbAg [12] molecules in the $X^2\Sigma^+$ ground electronic state have been proposed as promising candidates for precision measurements and electron electric dipole moment searches. While RaAg molecules are expected to be more sensitive than YbAg ones due to a larger nuclear charge of Ra than Yb, the formation and application of YbAg molecules may be advantageous because there already exist well-established experimental schemes of laser cooling, trapping, manipulation, and photoassociation of Yb atoms [13–15]. At the same time, molecules consisting of an Ag atom interacting with an alkali-metal or alkaline-earth-metal atom [16] have been shown to be strongly bound with highly polarized covalent or ionic bonds resulting in very large permanent electric dipole moments, significantly larger than in alkali-metal molecules. The RaAg molecule has been predicted to have the permanent electric dipole moment as large as $5.1D$ at the equilibrium distance and the potential well depth of 9563 cm^{-1} [16].

To the best of our knowledge, the electronic structure calculations for the YbAg molecule and the analogous YbCu and YbAu molecules have not yet been reported in the literature.

In this paper, to fill this gap and to facilitate the formation of such molecules for ultracold studies, we theoretically investigate the ground-state electronic properties of the YbCu, YbAg, and YbAu molecules. We compute potential energy curves, permanent electric dipole and quadrupole moments, and static electric dipole polarizabilities. We employ large Gaussian basis sets and the coupled cluster method restricted to single, double, and noniterative triple excitations to include the electron correlation. We use the small-core energy-consistent pseudopotentials to account for the scalar relativistic effects. We find that the studied molecules are relatively strongly bound and have large permanent dipole moments of $3.2D$, $3.3D$, and $5.3D$ at equilibrium distances for YbCu, YbAg and YbAu, respectively. The investigated molecules are chemically reactive unless segregated in an optical lattice or shielded with external fields.

The considered ultracold molecules can be formed from ultracold mixtures of closed-shell Yb and open-shell Cu, Ag, or Au atoms, following recent experimental advances in studies of Yb + Rb [17], Hg + Rb [18], Sr + Rb [19], Yb + Li [20], and Yb + Cs [21, 22] combinations. Both photoassociation [23] and magnetoassociation [24] followed by the stimulated Raman adiabatic passage stabilization [25] to the ground rovibrational level can potentially be employed. Bose–Einstein condensation [13] and degenerate Fermi gases [14] of Yb have already been realized. Cu and Ag atoms have also been produced and trapped at ultralow temperatures using buffer-gas cooling and magnetic trapping [26] or magneto-optical cooling and trapping [27]. Ultracold Au atoms may be obtained similarly but using UV lasers.

The structure of the paper is the following. In section 2, we describe the employed computational methods. In section 3, we present and discuss the obtained results. In section 4, we provide a summary and outlook.

2. Computational methods

We calculate potential energy curves in the Born–Oppenheimer approximation using the computational scheme recently applied to the ground electronic states of diatomic molecules consisting of a Cu or Ag atom interacting with an alkaline-earth-metal atom [16]. The interaction of a closed-shell Yb atom in the ground singlet 1S electronic state with an open-shell Cu, Ag, or Au atom in the lowest doublet 2S state results in the ground molecular electronic state of the doublet $X^2\Sigma^+$ symmetry.

The considered ground-state molecules are well described at all internuclear distances by single-reference methods. Therefore, we describe them with the spin-restricted open-shell coupled cluster method restricted to single, double, and non-iterative triple excitations (RCCSD(T)) [28, 29]. The interaction energies $V(R)$, as functions of the internuclear distance R , are obtained with the supermolecular method with the basis set superposition error (BSSE) corrected by using the Boys–Bernardi counterpoise correction [30],

$$V(R) = E_{AB}(R) - E_A(R) - E_B(R), \quad (1)$$

where $E_{AB}(R)$ is the total energy of the molecule AB, and $E_A(R)$ and $E_B(R)$ are the total energies of the atoms A and B computed in the diatom basis set, all at a distance R .

The topology of three-dimensional potential energy surfaces for the lowest $^2A'$, $^1A'$, and $^3A'$ electronic states of triatomic Yb₂A and YbA₂ molecules (A = Cu, Ag, Au) is studied using the second-order many-body (Møller–Plesset) perturbation theory [31]. Next, geometries and energies are optimized with the CCSD(T) method around global and local minima. BSSE is corrected by using the counterpoise correction.

The scalar relativistic effects are included by employing the relativistic effective-core energy-consistent pseudopotentials (ECP) to replace the inner-shell electrons [32]. The Cu, Ag, and Au atoms are described with the ECP10MDF, ECP28MDF, and ECP60MDF pseudopotentials [33], respectively, together with the aug-cc-pwCV5Z-PP basis sets designed for those ECPs [34] (i and h exponents are omitted because of incompatibility with CPP). The Yb atom is described with the ECP60MDF effective-core pseudopotential together with the corresponding core-polarization potential (CPP) [35] and the [10s10p9d5f3g] basis set [36]. Thus, 10, 28, 60 and, 60 electrons in the inner shells are replaced by pseudopotentials, and remaining $3s^23p^63d^{10}4s^1$, $4s^24p^64d^{10}5s^1$, $5s^25p^65d^{10}6s^1$, and $5s^25p^66s^2$ electrons from Cu, Ag, Au, and Yb, respectively, are treated explicitly and correlated. To accelerate the convergence toward the complete basis set limit, the atomic basis sets are additionally augmented in all calculations for diatomic molecules by the set of the [3s3p2d2f1g] bond functions [37].

The long-range dispersion-interaction $C_6^{\text{disp}} = \frac{3}{\pi} \int_0^\infty \alpha_A(i\omega)\alpha_B(i\omega)d\omega$ coefficients are calculated from the atomic dynamic electric dipole polarizabilities at the imaginary frequency, $\alpha_{A(B)}(i\omega)$ [44]. The dynamic polarizabilities of the Cu, Ag, and Au atoms are constructed as a sum over states using experimental

Table 1. Characteristics of the Cu, Ag, Au, and Yb atoms: the static electric dipole polarizability α , the ionization potential IP, the electron affinity EA, and the lowest $S-P$ excitation energy ($^2S-^2P$ for Cu, Ag, and Au and $^1S-^3P$ for Yb). Present theoretical values are compared with the most accurate available experimental or theoretical data. Experimental excitation energies are averaged on spin-orbit manifolds.

Atom	α ($e^2 a_0^3 / E_h$)	IP (cm^{-1})	EA (cm^{-1})	$S-P$ (cm^{-1})
Cu	45.9	62 406	10 003	31 062
	46.5 [38]	62 317 [39]	9967 [40]	30 701 [39]
Ag	50.2	61 249	10 608	30 363
	52.5 [38]	61 106 [39]	10 521 [40]	30 166 [39]
Au	36.3	74 216	18 519	40 632
	36.1 [38]	74 409 [39]	18 620 [41]	39 903 [39]
Yb	136.0	50 479	≈ 0	20 119
	139.3 [42]	50 443 [39]	≈ 0 [43]	18 869 [39]

Table 2. Characteristics of the YbCu, YbAg, and YbAu molecules in the $X^2\Sigma^+$ ground electronic state: equilibrium interatomic distance R_e , well depth D_e , harmonic constant ω_e , rotational constant B_e , permanent electric dipole moment d_e , permanent electric quadrupole moment Q_e , isotropic and anisotropic components of the static electric dipole polarizability $\bar{\alpha}_e$ and $\Delta\alpha_e$, and number of vibrational levels N_v .

Molecule	$R_e(a_0)$	D_e (cm^{-1})	ω_e (cm^{-1})	B_e (cm^{-1})	d_e (D)	Q_e (ea_0^2)	$\bar{\alpha}_e$ ($\frac{e^2 a_0^3}{E_h}$)	$\Delta\alpha_e$ ($\frac{e^2 a_0^3}{E_h}$)	N_v
YbCu	5.500	5708	144.3	0.0502	3.22	-0.80	182	100	84
YbAg	5.788	5253	109.4	0.0271	3.30	0.51	191	121	105
YbAu	5.554	13 349	125.0	0.0211	5.31	-0.23	152	55	183

energies [39] and transition dipole moments from references [45, 46]. The dynamic polarizability of the Yb atom is obtained with the explicitly connected representation of the expectation value and polarization propagator within the coupled cluster method [47]. The long-range dispersion-interaction C_8^{disp} coefficients are estimated by fitting the $-C_6^{\text{disp}}/R^6 - C_8^{\text{disp}}/R^8$ formula with the calculated C_6^{disp} coefficients to the calculated interaction potentials at interatomic distances between 12 and 30 bohr.

The permanent electric dipole $d(R)$ and quadrupole $Q(R)$ moments and static electric dipole polarizabilities $\alpha(R)$ are calculated with the finite field approach. The z axis is selected along the internuclear axis, oriented from the Cu, Ag, or Au atom to the Yb atom. The vibrationally averaged dipole moments d_v are calculated as expectation values with radial vibrational wavefunctions.

To validate the accuracy of the employed electronic structure method and basis sets, we calculate the atomic properties such as the static electric dipole polarizabilities, the ionization potentials, the electron affinities, and the lowest electronic excitation energies for the considered atoms and compare them with the most accurate available experimental or theoretical data in table 1. The very good agreement around 1% for most properties suggests that high accuracy of molecular calculations with the present methods can also be expected. Based on the quality of atomic assessment, test molecular calculations in smaller basis sets, and our previous experience, we estimate the uncertainty of the present results to be of the order of 5%.

All electronic structure calculations are performed with the Molpro package of *ab initio* programs [48, 49]. Vibrational eigenstates $\varphi_v(R)$ and eigenenergies E_v are computed using numerically exact diagonalization of the Hamiltonian for the nuclear motion within the discrete variable representation on the non-equidistant grid [50]. Atomic masses of the most abundant isotopes are assumed.

3. Results and discussion

3.1. Potential energy curves

The computed potential energy curves of the $X^2\Sigma^+$ symmetry for the YbCu, YbAg, and YbAu molecules are presented in figure 1. The corresponding spectroscopic characteristics such as the equilibrium interatomic distance R_e , well depth D_e , harmonic constant ω_e , rotational constant B_e , and number of vibrational levels N_v (for $j = 0$) are collected in table 2.

All potential energy curves presented in figure 1 show a smooth behavior with well-defined minima. The potential energy curves of the YbCu and YbAg molecules are similar to each other, whereas the binding in the YbAu molecule is significantly stronger. This difference can be attributed to a significantly larger electronegativity (by the Pauling scale [51]) of the Au (2.54) atom than that of the Cu (1.90) and Ag (1.93) atoms. The YbCu and YbAg molecules have slightly smaller well depths, while the YbAu molecule has a

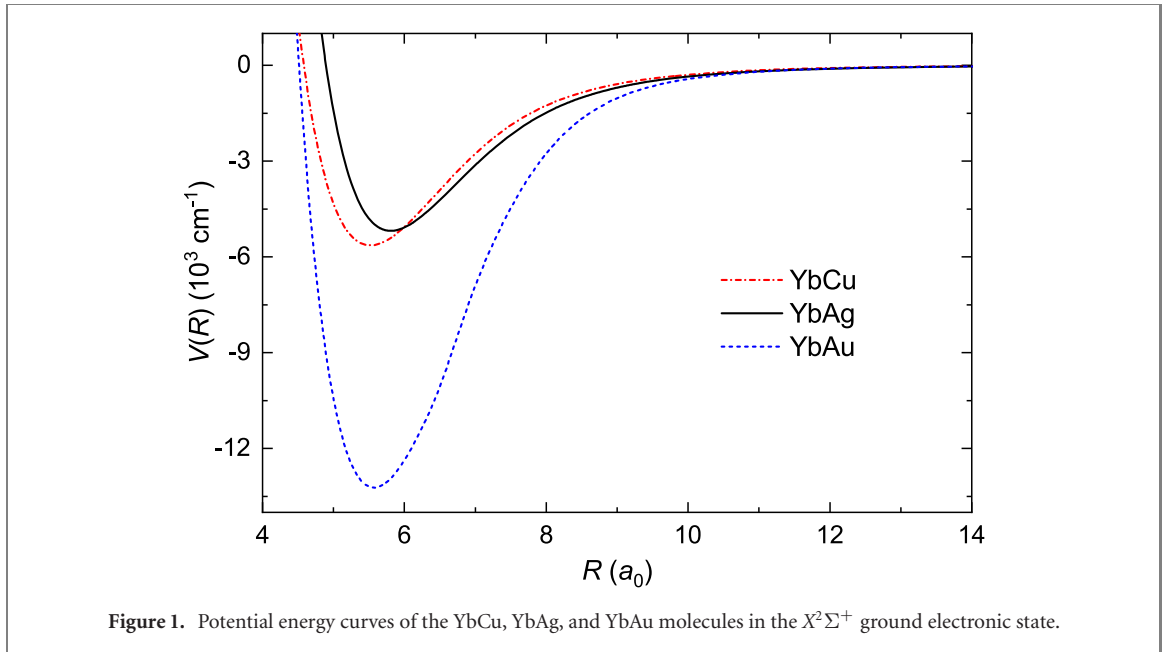


Figure 1. Potential energy curves of the YbCu, YbAg, and YbAu molecules in the $X^2\Sigma^+$ ground electronic state.

Table 3. Long-range C_6^{disp} and C_8^{disp} coefficients for interatomic interactions and long-range \tilde{C}_3^{dd} , \tilde{C}_4^{dq} , $\tilde{C}_6^{\text{disp}}$, and \tilde{C}_6^{rot} coefficients for intermolecular interactions.

Molecule	$C_6^{\text{disp}} (E_h a_0^6)$	$C_8^{\text{disp}} (E_h a_0^8)$	$\tilde{C}_3^{\text{dd}} (E_h a_0^3)$	$\tilde{C}_4^{\text{dq}} (E_h a_0^4)$	$\tilde{C}_6^{\text{disp}} (E_h a_0^6)$	$\tilde{C}_6^{\text{rot}} (E_h a_0^6)$
YbCu	629	7.5×10^4	1.60	-1.01	3190	1.9×10^6
YbAg	681	11×10^4	1.69	0.66	3429	3.8×10^6
YbAu	563	12×10^4	4.36	-0.48	2434	3.3×10^7

slightly larger well depth than the molecules consisting of an Ag or Cu atom interacting with an alkaline-earth-metal atom [16]. All three studied molecules are significantly more strongly bound and have shorter equilibrium distances than alkali-metal-ytterbium [52] and alkali-metal-alkaline-earth-metal molecules [53].

The relatively large binding energy and short equilibrium distances of the ground-state YbAu molecule may indicate the highly polarized covalent or even ionic nature of its chemical bond and significant stabilizing contribution of the electrostatic and induction interactions. The large difference in the electronegativity of the Au (2.54) and Yb (1.1) atoms may be responsible for a significant bond polarization and considerable contribution of the Yb^+Au^- ionic configuration to its ground state bonding [51]. This is further analyzed in the following subsection.

The interaction potentials at large interatomic distances approach asymptotic behavior given by

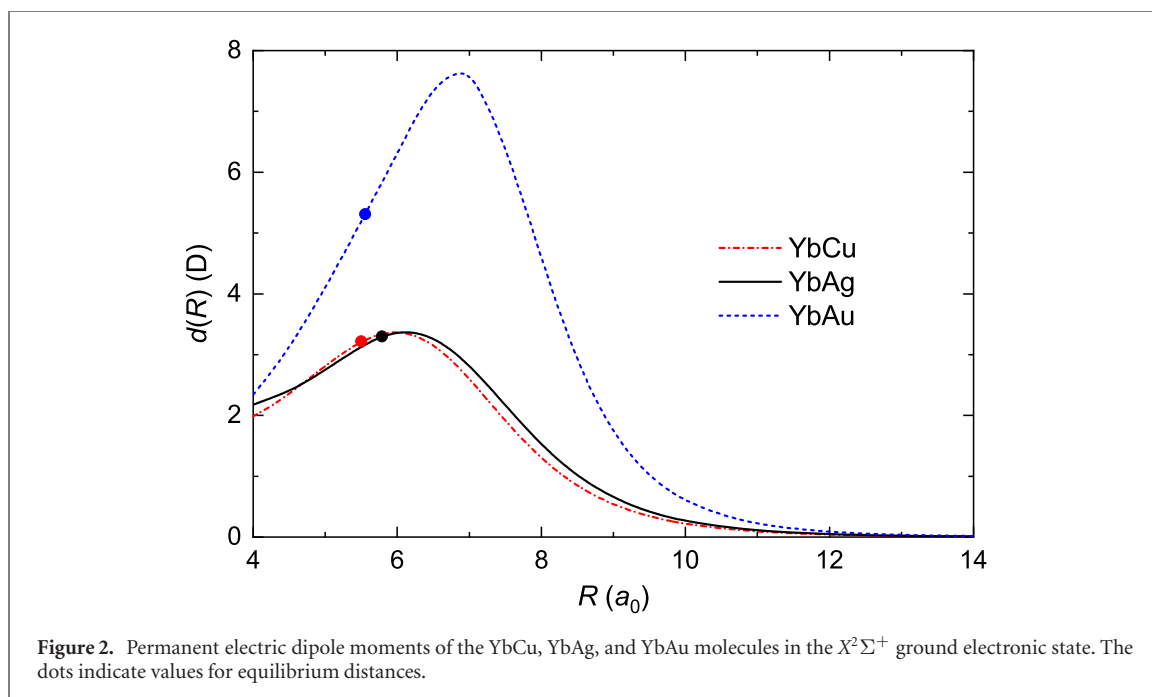
$$V(R) \approx -\frac{C_6^{\text{disp}}}{R^6} - \frac{C_8^{\text{disp}}}{R^8} + \dots, \quad (2)$$

where C_6^{disp} and C_8^{disp} are two leading long-range dispersion-interaction coefficients. The calculated coefficients for the studied systems are collected in table 3 and are smaller than for analogous alkali-metal and alkaline-earth-metal molecules because the polarizabilities of the Cu, Ag, and Au atoms are a few times smaller than the polarizabilities of alkali-metal and alkaline-earth-metal atoms.

3.2. Permanent electric dipole and quadrupole moments

Permanent electric dipole moments $d(R)$ as functions of the interatomic distance for the YbCu, YbAg, and YbAu molecules in the $X^2\Sigma^+$ ground electronic states are presented in figure 2. The corresponding values at equilibrium distances $d_e \equiv d(R_e)$ are collected in table 2.

The permanent electric dipole moment curves of the YbCu and YbAg molecules are similar to each other (similarly to potential energy curves), whereas the charge polarization in the YbAu molecule is significantly stronger. Again, this difference can be attributed to a significantly larger electronegativity of the Au atom than that of the Cu and Ag atoms. Permanent electric dipole moments can be used to measure the bond polarization and ionic character IC of the studied molecules, e.g. by calculating the ratio of the permanent electric dipole moment of a given molecule, d_e , at the equilibrium distance, R_e , to the maximal



possible value, $d_{\max} = eR_e$, corresponding to a purely ionic molecule [51],

$$\text{IC} = \frac{d_e}{d_{\max}} = \frac{d_e}{eR_e}. \quad (3)$$

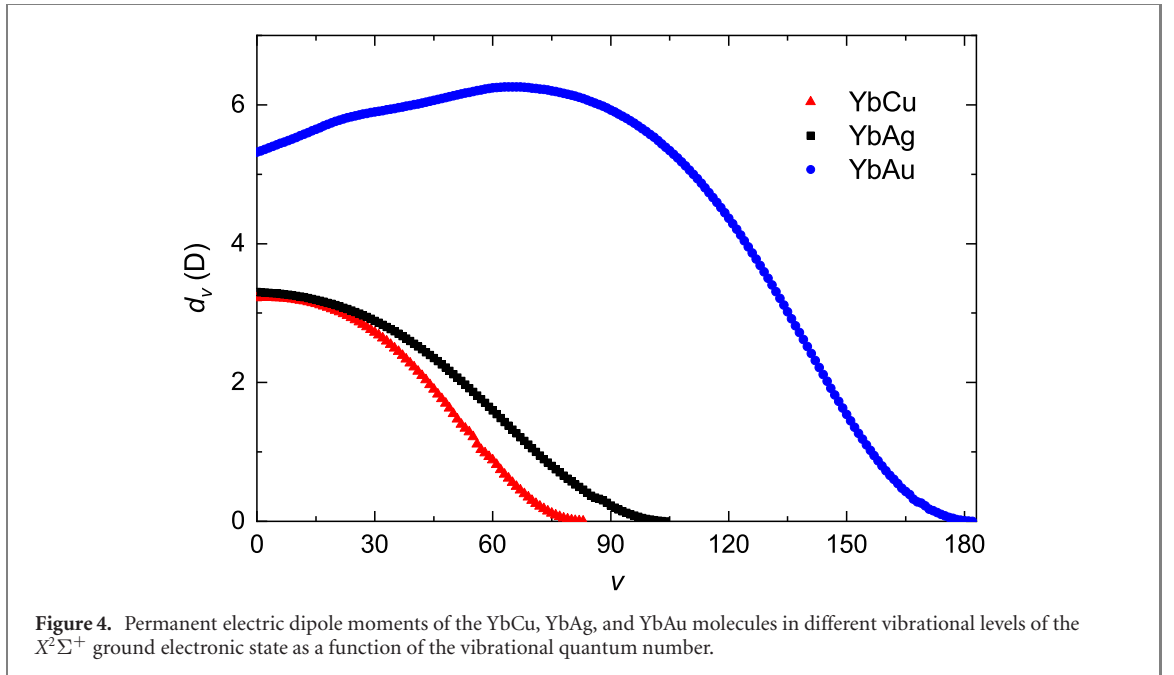
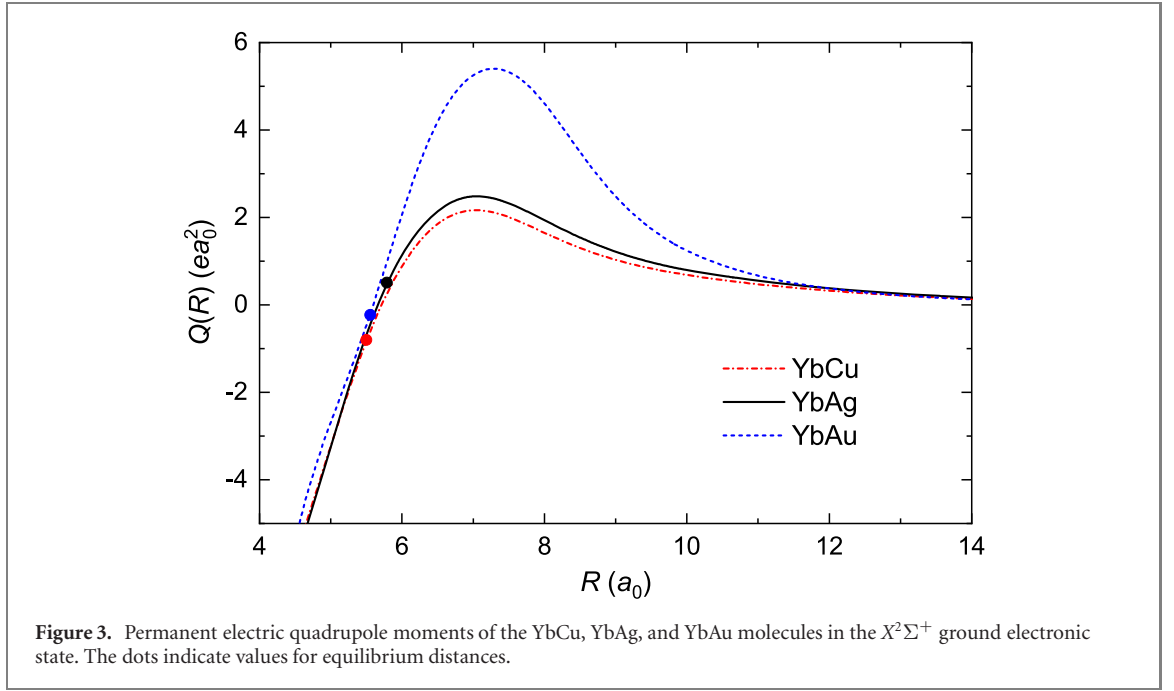
The calculated ratios are 23%, 22%, and 38% for YbCu, YbAg, and YbAu, respectively. These values agree with Mulliken and natural orbital population analysis [54]. Thus, the bonds in the YbCu and YbAg molecules are considerably polarized, whereas, in the YbAu molecule, the admixture of the Yb^+Au^- ionic configuration in the ground state may be significant. The observed trends coincide with the differences in atomic electronegativities χ of the Cu (1.90), Ag (1.93), Au (2.54), and Yb (1.1) atoms. The calculated ratios also agree with the approximate percent ionic character of a heteronuclear diatomic molecule with a single bond given by Pauling [51] $1 - \exp[-(\chi_{\text{Cu/Ag/Au}} - \chi_{\text{Yb}})]$, resulting in 18%, 19%, and 30% for YbCu, YbAg, and YbAu, respectively. The permanent electric dipole moment of YbAu increases linearly with the interatomic distance in the vicinity of the interaction potential well, additionally confirming its partially ionic character.

The YbCu, YbAg, and YbAu molecules have permanent electric dipole moments significantly larger than alkali-metal-ytterbium [52] and alkali-metal-alkaline-earth-metal molecules [53], but similar to molecules consisting of an Ag or Cu atom interacting with an alkaline-earth-metal atom [16]. The YbAu molecule has the permanent electric dipole moment as large as the most polar alkali-metal LiCs molecule [55].

The permanent electric quadrupole moments $Q(R)$ as functions of the interatomic distance for the YbCu, YbAg, and YbAu molecules in the $X^2\Sigma^+$ ground electronic states are presented in figure 3. Again, curves for the YbCu and YbAg molecules are similar to each other. The corresponding values at equilibrium distances $Q_e \equiv Q(R_e)$ are collected in table 2. The calculated quadrupole moments are relatively small, especially around equilibrium distances, where quadrupole moment curves change the sign.

The permanent electric dipole moments of the YbCu, YbAg, and YbAu molecules in different vibrational levels of their ground electronic state $d_v = \int |\varphi_v(R)|^2 d(R) dR$ as a function of the vibrational quantum number v are presented in figure 4. For YbCu, the largest value is 3.22D in the level with $v = 3$ and $E_b = -5208 \text{ cm}^{-1}$. For YbAg, the largest value is 3.30D in the level with $v = 0$ and binding energy $E_b = -5199 \text{ cm}^{-1}$. For YbAu, the largest value is 6.26D in the level with $v = 65$ and $E_b = -5756 \text{ cm}^{-1}$, while it is 5.33D in the level with $v = 0$ and $E_b = -13287 \text{ cm}^{-1}$. The increase of the permanent electric dipole moment with increasing the vibrational quantum number and decreasing the vibrational binding energy is visible for the YbAu molecule with $v < 65$ due to the observed increase of its permanent electric dipole moment with the interatomic distance (cf figure 2). Thus, large permanent electric dipole moments for YbAu molecules in highly excited vibrational levels may allow for new molecular control schemes.

The relatively large permanent electric dipole moments combined with large reduced masses and small rotational constants of the investigated molecules open the way for their applications in quantum



simulations of strongly interacting dipolar quantum many-body systems, controlled chemistry, and precision measurements. Such applications often require molecular polarization with the external static electric field. The characteristic scale of the electric field needed to polarize molecules can be quantified by

$$\mathcal{E}_{\text{pol}} = \frac{2B_e}{d_e}. \quad (4)$$

Values of the polarizing electric field for the YbCu, YbAg, and YbAu molecules are presented in table 4, together with values for other molecules relevant for ongoing ultracold experiments. For the YbAg molecule, \mathcal{E}_{pol} is below 1 kV cm^{-1} , which is smaller and more favorable than for most of the other ultracold molecules.

The intermolecular interactions between the studied molecule at ultralow temperatures are dominated by the long-range dipolar interaction, which for the polarized molecules takes the form

$$V_{\text{dd}}(R, \theta) = \frac{\tilde{C}_3^{\text{dd}}(1 - 3 \cos^2 \theta)}{R^3}, \quad (5)$$

Table 4. Characteristics of dipolar molecules and their intermolecular interactions: ground-state permanent electric dipole moment d_e , polarizing electric field \mathcal{E}_{pol} , characteristic length of dipolar interaction a_{dd} , and characteristic nearest-neighbor energy shift $V_{\text{dd}} = C_3^{\text{dd}}/(\lambda/2)^3$ for molecules in an optical lattice formed by $\lambda = 1064$ nm laser. Results for the YbCu, YbAg, and YbAu molecules are compared with parameters for other molecules used in ultracold experiments [56].

Molecule	d_e (D)	\mathcal{E}_{pol} (V cm $^{-1}$)	a_{dd} ($10^3 a_0$)	V_{dd} (kHz)
YbCu	3.22	1860	231	10.4
YbAg	3.30	978	288	10.9
YbAu	5.31	474	982	28.2
CsAg [16]	9.75	329	2144	95.3
KRb [57]	0.57	7832	4	0.3
NaRb [58]	3.2	2594	106	10.3
LiCs [59]	5.5	4071	398	30.3
RbSr [60]	1.5	1467	37	2.3
CaF [61]	3.1	13 287	52	9.4

where θ is the angle between the directions of polarization and intermolecular axis, and the long-range dipole–dipole electrostatic-interaction coefficient \tilde{C}_3^{dd} is given by

$$\tilde{C}_3^{\text{dd}} = \frac{d_v^2}{4\pi\epsilon_0}, \quad (6)$$

where d_v is the permanent electric dipole moment of molecules in a state v . The \tilde{C}_3^{dd} coefficients for the studied ground-state molecules are collected in table 3.

The dipole–dipole interactions can be further characterized by an effective dipolar length a_{dd} [62] defined by

$$a_{\text{dd}} = \frac{d_v^2 m}{12\pi\epsilon_0 \hbar^2}, \quad (7)$$

where m is the molecule mass. The dipolar lengths for the studied ground-state molecules are collected in table 4 and compared with values for other molecules relevant for ongoing ultracold experiments. They are significantly larger for the present molecules than for other $^2\Sigma$ -state molecules and comparable to the most dipolar alkali-metal molecules.

Another important parameter characterizing dipole-dipole interactions is the energy shift between nearest-neighbor molecules in an optical lattice $V_{\text{dd}} = C_3^{\text{dd}}/(\lambda/2)^3$, where λ is the laser wavelength. Its values for the studied ground-state molecules are collected in table 4 and compared with values for other molecules relevant for ongoing ultracold experiments. Again, they are comparable or larger for the present molecules than for other molecules.

Higher-order electrostatic terms of intermolecular interactions with more complex orientation dependences include the dipole–quadrupole $\sim d_v Q_v/R^4$, quadrupole–quadrupole $\sim Q_v^2/R^5$, and dipole–octupole $\sim d_v O_v/R^5$ contributions [63]. The long-range dipole–quadrupole electrostatic-interaction coefficients,

$$\tilde{C}_4^{\text{dq}} = \frac{d_v Q_v}{4\pi\epsilon_0}, \quad (8)$$

for the studied ground-state molecules are also collected in table 3, but have small valued because of small molecular quadrupole moments.

If molecules are not polarized by an external electric field, then in their ground rotational states, their interaction is dominated by the effective isotropic term $-\tilde{C}_6^{\text{rot}}/R^6$, resulting from the dipolar interaction in the second-order of perturbation theory and given by the long-range coefficient

$$\tilde{C}_6^{\text{rot}} = \frac{d_v^4}{6B_v}, \quad (9)$$

where B_v is the rotational constant for a vibrational state v . The \tilde{C}_6^{rot} coefficients for the studied ground-state molecules are collected in table 3.

3.3. Static electric dipole polarizabilities

The computed parallel $\alpha^{\parallel}(R) \equiv \alpha^{zz}(R)$ and perpendicular $\alpha^{\perp}(R) \equiv \alpha^{xx}(R) = \alpha^{yy}(R)$ components of the static electric dipole polarizability tensor as functions of the interatomic distance for the YbCu, YbAg, and YbAu molecules in the $X^2\Sigma^+$ electronic states are presented in figure 5(a). The polarizabilities for YbCu and

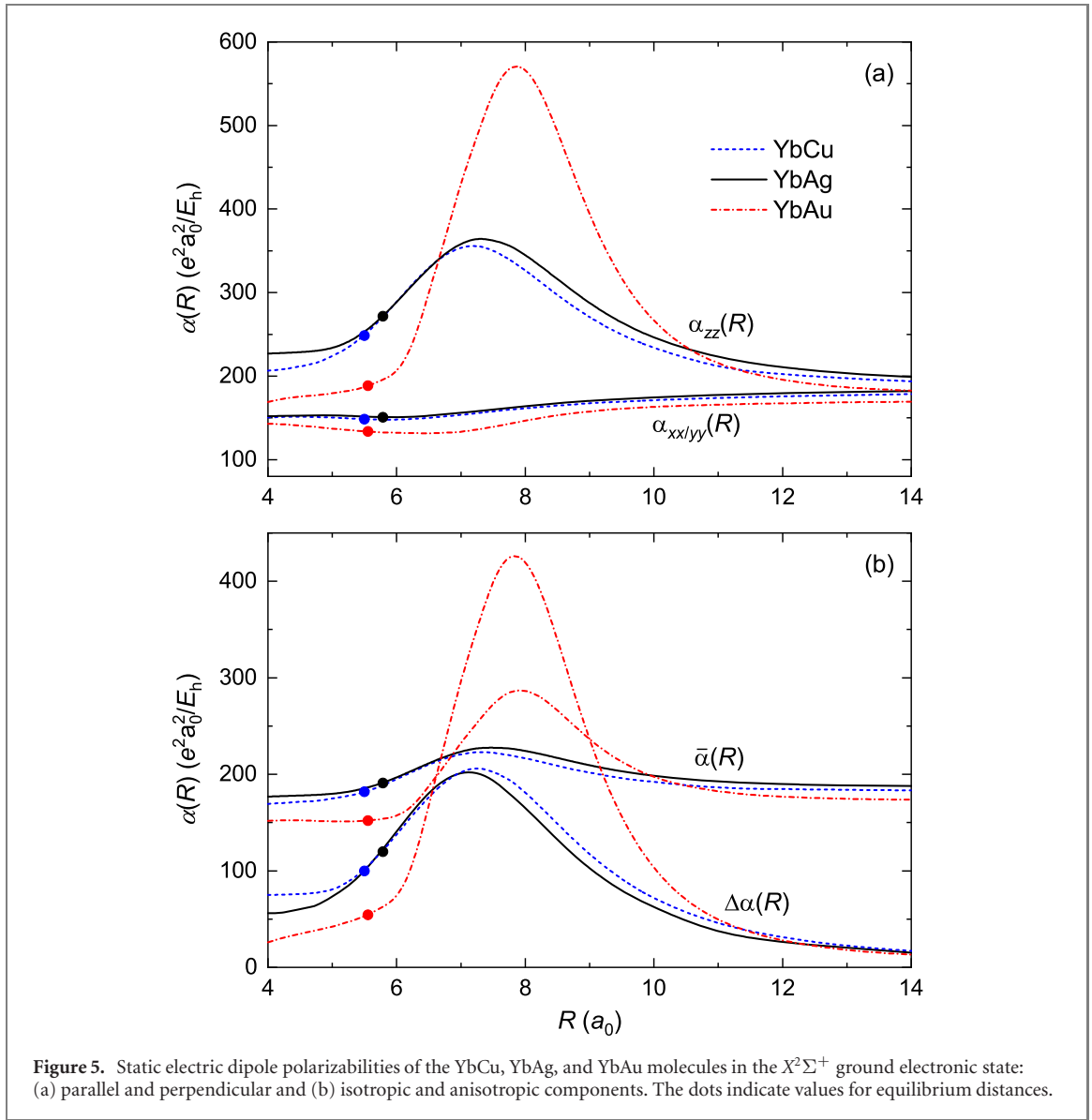


Figure 5. Static electric dipole polarizabilities of the YbCu, YbAg, and YbAu molecules in the $X^2\Sigma^+$ ground electronic state: (a) parallel and perpendicular and (b) isotropic and anisotropic components. The dots indicate values for equilibrium distances.

YbAg are similar to each other, while the interaction-induced variation for YbAu is much more pronounced. At large interatomic distances, they approach their asymptotic behavior given by the atomic polarizabilities α_A and α_B [64]

$$\begin{aligned}\alpha^{\parallel}(R) &\approx \alpha_A + \alpha_B + \frac{4\alpha_A\alpha_B}{R^3} + \frac{4(\alpha_A + \alpha_B)\alpha_A\alpha_B}{R^6}, \\ \alpha^{\perp}(R) &\approx \alpha_A + \alpha_B - \frac{2\alpha_A\alpha_B}{R^3} + \frac{(\alpha_A + \alpha_B)\alpha_A\alpha_B}{R^6}.\end{aligned}\quad (10)$$

The isotropic $\bar{\alpha}(R)$ and anisotropic $\Delta\alpha(R)$ components of the static electric dipole polarizability can also be obtained from $\alpha^{\perp}(R)$ and $\alpha^{\parallel}(R)$

$$\begin{aligned}\bar{\alpha}(R) &= \frac{2\alpha^{\perp}(R) + \alpha^{\parallel}(R)}{3}, \\ \Delta\alpha(R) &= \alpha^{\parallel}(R) - \alpha^{\perp}(R).\end{aligned}\quad (11)$$

They are presented in figure 5(b). Their values at the equilibrium distances, $\bar{\alpha}_e \equiv \bar{\alpha}(R_e)$ and $\Delta\alpha_e \equiv \Delta\alpha(R_e)$, are collected for the studied molecules in table 2. The equilibrium values are relatively close to the asymptotic ones, despite a large variation of the calculated polarizabilities at intermediate distances, especially for the YbAu molecule.

The polarizability describes the molecular response to the electric field in the second order of perturbation theory. For example, optical dipole trapping is governed by the isotropic polarizability $\bar{\alpha}$,

while the laser-induced molecular alignment is controlled by the anisotropy of the polarizability $\Delta\alpha$ [65]. Molecular polarizabilities may also be useful in the evaluation of intermolecular interactions [44].

The leading long-range dispersion-interaction coefficients can be estimated by combination rules, e.g. by the Slater–Kirkwood approximation [66],

$$C_{6,ij}^{\text{disp}} \approx \frac{2}{3} \frac{\alpha_i \alpha_j}{(\alpha_i/N_i)^{1/2} + (\alpha_j/N_j)^{1/2}}, \quad (12)$$

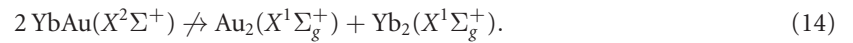
where $\alpha_{i(j)}$ is the static electric dipole polarizability of the $i(j)$ monomer and $N_{i(j)}$ represents its effective number of electrons. The effective number of electrons can be roughly approximated by the number of valence electrons or calculated from the known coefficients between like monomers, resulting in another known expression [67]

$$C_{6,ij}^{\text{disp}} \approx \frac{2\alpha_i \alpha_j C_{6,ii}^{\text{disp}} C_{6,jj}^{\text{disp}}}{\alpha_i^2 C_{6,jj}^{\text{disp}} + \alpha_j^2 C_{6,ii}^{\text{disp}}}. \quad (13)$$

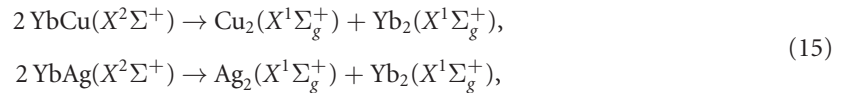
Both equations (12) and (13) reproduce exact interatomic C_6^{disp} coefficients for YbAg, YbCu, and YbAu with accuracy better than 10%. Therefore, we calculate the intermolecular long-range dispersion-interaction coefficients $\tilde{C}_6^{\text{disp}}$ between ground-state molecules using equation (12) with the isotropic polarizabilities $\bar{\alpha}_e$ and the effective number of electrons $N = 3$ and collect them in table 3. The values for the YbCu and YbAg molecules agree within 10% with the rough approximation neglecting intramolecular interactions, $\tilde{C}_6^{\text{disp}} \approx 2C_{6,\text{YbA}}^{\text{disp}} + C_{6,\text{A}_2}^{\text{disp}} + C_{6,\text{Yb}_2}^{\text{disp}}$ (the agreement for the YbAu molecule is worse because of its highly polarized bond). The calculated intermolecular electronic dispersion $\tilde{C}_6^{\text{disp}}$ coefficients are, however, negligibly small as compared to the rotational \tilde{C}_6^{rot} ones (cf table 3).

3.4. Chemical reactions

The stability of the studied molecules against chemical reactions may be assessed using the calculated potential well depths and related dissociation energies [36, 68, 69]. Among the investigated species, the most-strongly-bound YbAu molecules in the rovibrational ground state of the $X^2\Sigma^+$ ground electronic state are chemically stable against atom-exchange reactions, i.e.

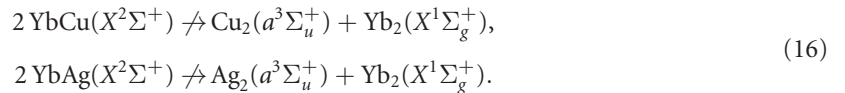


On the other hand, two other molecules are chemically reactive



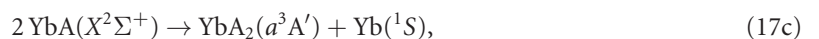
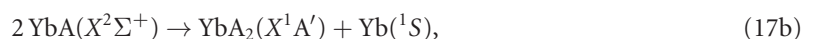
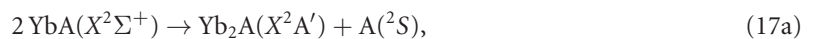
because the binding of the Cu_2 and Ag_2 dimers [16] is much stronger than that of the YbCu and YbAg molecules.

The chemical reactivity of the YbCu and YbAg molecules may potentially be suppressed by spin-polarizing molecules with an external magnetic field, restricting the collision dynamics to high-spin intermolecular interaction potentials [69]. In the triplet state, the following atom-exchange reactions are energetically forbidden



Unfortunately, the spin-relaxation mediated by the magnetic spin-spin and second-order spin-orbit coupling may lead to reactive singlet intermolecular interaction potentials [70, 71].

Except for the atom-exchange reactions, the trimer formation reactions may be another path of chemical losses [36, 68, 69]:



with $A = \text{Cu}, \text{Ag}, \text{or Au}$. Depending on the topology of potential energy surfaces, the $^1A'$ and $^2A'$ electronic states coreduce to 1A_1 and 2A_1 for isosceles triangular equilibrium geometries or $^1\Sigma^+$ and $^2\Sigma^+$ for linear ones, whereas the $^3A'$ electronic state coreduce to 3B_2 for isosceles triangular equilibrium geometry. Results of electronic structure calculations for triatomic Yb_2A and YbA_2 molecules are collected in table 5. We find that the reactions (17a) leading to the linear $\text{YbAYb}(^2\Sigma_g^+)$ molecules are energetically suppressed for all the

Table 5. Characteristics of the triatomic Yb₂A and YbA₂ molecules (A = Cu, Ag, Au): electronic state symmetry, equilibrium angle formed by ABC atoms θ_e^{ABC} , equilibrium distance between A and B atoms R_e^{AB} , equilibrium distance between B and C atoms R_e^{BC} , and well depth D_e .

ABC	Symm.	θ_e^{ABC} (deg.)	R_e^{AB} (a_0)	R_e^{BC} (a_0)	D_e (cm^{-1})
YbCuYb	$^2\Sigma_g^+$	180	5.79	5.79	8792
YbCuCu	$^1\Sigma_g^+$	180	5.68	4.26	20217
CuYbCu	$^1\Sigma_g^+$	180	5.43	5.43	19213
CuYbCu	3B_2	45.7	5.70	5.70	15850
YbAgYb	$^2\Sigma_g^+$	180	6.04	6.04	8417
YbAgAg	$^1\Sigma_g^+$	180	5.92	4.84	17890
AgYbAg	$^1\Sigma_g^+$	180	5.71	5.71	18034
AgYbAg	3B_2	50.7	5.97	5.97	13873
YbAuYb	$^2\Sigma_g^+$	180	6.00	6.00	14757
YbAuAu	$^1\Sigma_g^+$	180	5.58	4.80	27857
AuYbAu	$^1\Sigma_g^+$	180	5.53	5.53	33913
AuYbAu	3B_2	50.6	5.84	5.84	26041

studied diatomic molecules in their ground states, while the reactions (17b) leading to the strongly bound linear AYbA($^1\Sigma_g^+$) or YbAA($^1\Sigma^+$) molecules are exothermic for all the studied diatomic molecules. The reactions (17c) leading to the isoscales triangular A₂Yb(3B_2) molecules are exothermic for YbCu and YbAg, while nearly thermoneutral for YbAu. The binding energies of trimers are large, mostly more than twice larger than that of YbA($X^2\Sigma^+$) dimers, because of stabilizing electrostatic and three-body interactions.

Finally, we check that there are no reaction barriers at minimum-energy reaction paths for all the considered above exothermic chemical reactions [69], which are unavoidable for all the investigated molecules, therefore all of them are chemically reactive even at ultralow temperatures. This opens the way for studying ultracold controlled chemical reactions. If chemical reactions are not desired, e.g. in precision measurements or quantum many-body simulations, then the molecules should be protected from binary collisions by segregation in an optical lattice or shielding with external electromagnetic fields. Shielding with a microwave field [72] or by polarizing with an external electric field in a reduced dimensionality [73] has already been experimentally demonstrated.

4. Summary and conclusions

Motivated by the experimental progress on formation and application of ultracold Yb + Rb [17], Hg + Rb [18], Sr + Rb [19], Yb + Li [20], and Yb + Cs [21, 22] mixtures and recent theoretical proposal for using ultracold YbAg molecules for electron electric dipole moment searches [12], we have studied electronic properties of the YbCu, YbAg, and YbAu molecules. We have calculated potential energy curves, permanent electric dipole and quadrupole moments, and static electric dipole polarizabilities using the coupled cluster method restricted to single, double, and noniterative triple excitations with large Gaussian basis sets and small-core energy-consistent pseudopotentials.

We have found that the studied molecules are relatively strongly bound and have relatively large permanent electric dipole moments. For YbAu, the maximal electric dipole moment exceeds $6.2D$ for highly excited vibrational level. We have also assessed possible channels of chemical reactions based on the energetics of the reactants and products and found that the considered molecules are chemically reactive. The investigated molecules may find application in ultracold controlled chemistry, dipolar many-body physics, or precision measurement experiments.

Full potential energy curves, permanent electric dipole moments, and electric dipole polarizabilities as a function of interatomic distance in a numerical form are collected in the supplemental material (<https://stacks.iop.org/NJP/23/085003/mmedia>). The excited electronic states should be studied in the future to guide the formation of the considered molecules via magnetoassociation [19, 20] followed by an optical stabilization or photoassociation [17, 21] using a $D1$ line in Cu, Ag, and Au or an intercombination line in Yb.

Acknowledgments

Financial support from the National Science Centre Poland (Grant No. 2015/19/D/ST4/02173) and the Foundation for Polish Science within the First Team program co-financed by the European Union under the

European Regional Development Fund is gratefully acknowledged. The computational part of this research has been partially supported by the PL-Grid Infrastructure.

Data availability statement

All data that support the findings of this study are included within the article (and any supplementary files).

ORCID iDs

Michał Tomza  <https://orcid.org/0000-0003-1792-8043>

References

- [1] Carr L D, DeMille D, Krems R V and Ye J 2009 *New J. Phys.* **11** 055049
- [2] Bohn J L, Rey A M and Ye J 2017 *Science* **357** 1002
- [3] Gross C and Bloch I 2017 *Science* **357** 995
- [4] DeMille D, Doyle J M and Sushkov A O 2017 *Science* **357** 990
- [5] Chupp T E, Fierlinger P, Ramsey-Musolf M J and Singh J T 2019 *Rev. Mod. Phys.* **91** 015001
- [6] Kobayashi J, Ogino A and Inouye S 2019 *Nat. Commun.* **10** 3771
- [7] Andreev V *et al* 2018 *Nature* **562** 355
- [8] Alighanbari S, Giri G S, Constantin F L, Korobov V I and Schiller S 2020 *Nature* **581** 152
- [9] Safronova M S, Budker D, DeMille D, Kimball D F J, Derevianko A and Clark C W 2018 *Rev. Mod. Phys.* **90** 025008
- [10] Fleig T and DeMille D (unpublished)
- [11] Sunaga A, Abe M, Hada M and Das B P 2019 *Phys. Rev. A* **99** 062506
- [12] Verma M, Jayich A M and Vutha A C 2020 *Phys. Rev. Lett.* **125** 153201
- [13] Takasu Y, Maki K, Komori K, Takano T, Honda K, Kumakura M, Yabuzaki T and Takahashi Y 2003 *Phys. Rev. Lett.* **91** 040404
- [14] Fukuhara T, Takasu Y, Kumakura M and Takahashi Y 2007 *Phys. Rev. Lett.* **98** 030401
- [15] Tojo S, Kitagawa M, Enomoto K, Kato Y, Takasu Y, Kumakura M and Takahashi Y 2006 *Phys. Rev. Lett.* **96** 153201
- [16] Smialkowski M and Tomza M 2021 *Phys. Rev. A* **103** 022802
- [17] Nemitz N, Baumer F, Münchow F, Tassy S and Görlitz A 2009 *Phys. Rev. A* **79** 061403
- [18] Witkowski M, Nagórny B, Munoz-Rodriguez R, Ciuryło R, Żuchowski P S, Bilicki S, Piotrowski M, Morzyński P and Zawada M 2017 *Opt. Express* **25** 3165
- [19] Barbé V, Ciamei A, Pasquiou B, Reichsöllner L, Schreck F, Żuchowski P S and Hutson J M 2018 *Nat. Phys.* **14** 881
- [20] Green A, Li H, See Toh J H, Tang X, McCormick K C, Li M, Tiesinga E, Kotochigova S and Gupta S 2020 *Phys. Rev. X* **10** 031037
- [21] Guttridge A, Hopkins S A, Frye M D, McFerran J J, Hutson J M and Cornish S L 2018 *Phys. Rev. A* **97** 063414
- [22] Wilson K E, Guttridge A, Segal J and Cornish S L 2021 *Phys. Rev. A* **103** 033306
- [23] Jones K M, Tiesinga E, Lett P D and Julienne P S 2006 *Rev. Mod. Phys.* **78** 483
- [24] Köhler T, Góral K and Julienne P S 2006 *Rev. Mod. Phys.* **78** 1311
- [25] Vitanov N V, Rangelov A A, Shore B W and Bergmann K 2017 *Rev. Mod. Phys.* **89** 015006
- [26] Brahm N, Newman B, Johnson C, Greytak T, Kleppner D and Doyle J 2008 *Phys. Rev. Lett.* **101** 103002
- [27] Uhlenberg G, Dirscherl J and Walther H 2000 *Phys. Rev. A* **62** 063404
- [28] Purvis G D III and Bartlett R J 1982 *J. Chem. Phys.* **76** 1910
- [29] Knowles P J, Hampel C and Werner H J 1993 *J. Chem. Phys.* **99** 5219
- [30] Boys S F and Bernardi F 1970 *Mol. Phys.* **19** 553
- [31] Amos R D, Andrews J S, Handy N C and Knowles P J 1991 *Chem. Phys. Lett.* **185** 256
- [32] Dolg M and Cao X 2012 *Chem. Rev.* **112** 403
- [33] Figgen D, Rauhut G, Dolg M and Stoll H 2005 *Chem. Phys.* **311** 227
- [34] Peterson K A and Puzzarini C 2005 *Theor. Chem. Acc.* **114** 283
- [35] Wang Y and Dolg M 1998 *Theor. Chem. Acc.* **100** 124
- [36] Smialkowski M and Tomza M 2020 *Phys. Rev. A* **101** 012501
- [37] Bond function exponents, s : 0.6, 0.2, 0.067, 0.02, p : 0.6, 0.2, 0.067, 0.02, d : 0.4, 0.13, 0.04 f : 0.4, 0.13, 0.04, g : 0.2
- [38] Neogrady P, Kellö V, Urban M and Sadlej A J 1997 *Int. J. Quantum Chem.* **63** 557
- [39] Alexander Kramida, Yuri Ralchenko, Joseph Reader and NIST ASD Team 2020 <http://physics.nist.gov/PhysRefData/ASD>
- [40] Bilodeau R C, Scheer M and Haugen H K 1998 *J. Phys. B: At. Mol. Opt. Phys.* **31** 3885
- [41] Hotop H and Lineberger W C 1973 *J. Chem. Phys.* **58** 2379
- [42] Beloy K 2012 *Phys. Rev. A* **86** 022521
- [43] Andersen T, Haugen H K and Hotop H 1999 *J. Phys. Chem. Ref. Data* **28** 1511
- [44] Jeziorski B, Moszynski R and Szalewicz K 1994 *Chem. Rev.* **94** 1887
- [45] Topcu S, Nasser J, Daku L M L and Fritzsche S *Phys. Rev. A* **73** 042503.
- [46] Zhang Y, Mitroy J, Sadeghpour H R and Bromley M W J 2008 *Phys. Rev. A* **78** 062710
- [47] Korona T, Przybytek M and Jeziorski B 2006 *Mol. Phys.* **104** 2303
- [48] Werner H-J *et al* 2012 MOLPRO, version 2012.1, a package of *ab initio* programs see <http://molpro.net>
- [49] Werner H-J, Knowles P J, Knizia G, Manby F R and Schütz M 2012 *Wiley Interdiscip. Rev.-Comput. Mol. Sci.* **2** 242
- [50] Tiesinga E, Williams C J and Julienne P S 1998 *Phys. Rev. A* **57** 4257
- [51] Pauling L 1960 *The Nature of the Chemical Bond* (Ithaca, NY: Cornell University Press)
- [52] Shao Q, Deng L, Xing X, Gou D, Kuang X and Li H 2017 *J. Phys. Chem. A* **121** 2187
- [53] Pototschnig J V, Hauser A W and Ernst W E 2016 *Phys. Chem. Chem. Phys.* **18** 5964
- [54] Reed A E, Weinstock R B and Weinhold F 1985 *J. Chem. Phys.* **83** 735

- [55] Aymar M and Dulieu O 2005 *J. Chem. Phys.* **122** 204302
- [56] Gadway B and Yan B 2016 *J. Phys. B: At. Mol. Opt. Phys.* **49** 152002
- [57] Ni K-K *et al* 2008 *Science* **322** 231
- [58] Guo M *et al* 2016 *Phys. Rev. Lett.* **116** 205303
- [59] Deiglmayr J, Grochola A, Repp M, Mörtlbauer K, Glück C, Lange J, Dulieu O, Wester R and Weidemüller M 2008 *Phys. Rev. Lett.* **101** 133004
- [60] Ciamei A *et al* 2018 *Phys. Chem. Chem. Phys.* **20** 26221
- [61] Truppe S, Williams H J, Hambach M, Caldwell L, Fitch N J, Hinds E A, Sauer B E and Tarbutt M R 2017 *Nat. Phys.* **13** 1173
- [62] Lahaye T, Menotti C, Santos L, Lewenstein M and Pfau T 2009 *Rep. Prog. Phys.* **72** 126401
- [63] Stone A 2013 *The Theory of Intermolecular Forces* (Oxford: Oxford University Press)
- [64] Jensen L, Åstrand P-O, Osted A, Kongsted J and Mikkelsen K V 2002 *J. Chem. Phys.* **116** 4001
- [65] Lemeshko M, Krems R V, Doyle J M and Kais S 2013 *Mol. Phys.* **111** 1648
- [66] Slater J C and Kirkwood J G 1931 *Phys. Rev.* **37** 682
- [67] Kramer H L and Herschbach D R 1970 *J. Chem. Phys.* **53** 2792
- [68] Żuchowski P S and Hutson J M 2010 *Phys. Rev. A* **81** 060703
- [69] Tomza M, Madison K W, Moszynski R and Krems R V 2013 *Phys. Rev. A* **88** 050701
- [70] Janssen L M C, van der Avoird A and Groenenboom G C 2013 *Phys. Rev. Lett.* **110** 063201
- [71] Hermsmeier R, Klos J, Kotochigova S and Tscherbul T V 2021 arXiv:2102.05707
- [72] Anderegg L, Burchesky S, Bao Y, Yu S S, Karman T, Chae E, Ni K-K, Ketterle W and Doyle J M 2021 arXiv:2102.04365
- [73] Matsuda K, De Marco L, Li J-R, Tobias W G, Valtolina G, Quéméner G and Ye J 2020 *Science* **370** 1324